International Journal of Ambient Energy

ISSN: 0143-0750 (Print) 2162-8246 (Online) Journal homepage: http://www.tandfonline.com/loi/taen20

A compromise between the Temperature Difference and Performance in a Standing Wave Thermoacoustic Refrigerator

Mahmoud Alamir & Ahmed A. Elamer

To cite this article: Mahmoud Alamir & Ahmed A. Elamer (2018): A compromise between the Temperature Difference and Performance in a Standing Wave Thermoacoustic Refrigerator, International Journal of Ambient Energy

To link to this article: https://doi.org/10.1080/01430750.2018.1517673

Accepted author version posted online: 29 Aug 2018.

Publisher: Taylor & Francis & Informa UK Limited, trading as Taylor & Francis Group

Journal: *International Journal of Ambient Energy*

DOI: 10.1080/01430750.2018.1517673

A compromise between the Temperature Difference and Performance in a Standing Wave Thermoacoustic Refrigerator

Keywords: DeltaEC; Performance; Refrigeration; Thermoacoustics; Temperature difference.

Highlights

- A theoretical DeltaEC model of a standing wave thermoacoustic refrigerator is built.
- Compromised values for the geometric parameters and operating conditions are collected.
- The physical description of the performance and the temperature difference change behavior is presented.

Abstract

Thermoacoustic refrigeration is an evolving cooling technology where the acoustic power is used to pump heat. The operating conditions and geometric parameters are important for the thermoacoustic refrigerator performance, as they affect both its performance and the temperature difference across the stack. This paper investigates the effect of the stack geometric parameters and operating conditions on the performance of a standing wave thermoacoustic refrigerator and the temperature difference across the stack. DeltaEC software is used to make the thermoacoustic refrigerator model. From the obtained results, normalised values for the operating conditions and geometric parameters are collected to compromise both the performance and the temperature difference across the stack.

1. Introduction

Thermoacoustic refrigeration is a developing cooling technology. It has many positives over other alternative refrigeration technologies, as it uses environment friendly working gases, the cooling capacity is continuously controlled, the design is simple, and it can operate quietly [1–3]. This cooling technology is now in the research and development process, and it is expected for noticeable spread commercially [4].

Thermoacoustic refrigeration uses the vibrational sound pressure waves. The heat is pumped from low temperature source to high temperature sink by the sound waves. Fig. 1 shows a typical standing wave thermoacoustic refrigerator. The function generator and the amplifier feed the signal to the acoustic driver, and transmit the required frequency and power into the resonator. Following this, the wave through the resonator produces hot and cold temperature regions due to the high and low-pressure areas distribution across the resonator. The stack which has low thermal conductivity separates the hot and cold areas inside the resonator, and two heat exchangers are bounded the stack for heat transfer.

Insert Fig. 1 about here.

The temperature difference is a key parameter in refrigeration area, as a large temperature difference may be required in some applications that need low temperatures. This can be on the expense of the performance or even the obtained cooling loads. Further, the operating conditions and geometric parameters of thermoacoustic refrigerators can have an influence on both the temperature difference across the stack and the consumed acoustic power. Therefore, the operating conditions and the geometric parameters should be compromised to give a desired temperature difference across the stack with a high performance.

Recently, researchers have shown an increased interest in optimizing thermoacoustic refrigerators. A number of researchers have reported design and optimization algorithms for the thermoacoustic devices. Wetzel and Herman [5] developed an algorithm for thermoacoustic refrigerators. The total acoustic power was introduced as follows,

$$\dot{W}_{tot} = \dot{W}_s + \dot{W}_{res} + \dot{W}_{hex} \quad (1)$$

Tijani [6] experimentally tested a loudspeaker driven thermoacoustic refrigerator. A simplified design flow chart for this refrigerators type was presented based on the effect of normalised stack parameters on the performance.

Babaei and Siddiqui [7] studied a general optimization algorithm for thermoacoustic devices. This algorithm was based on energy balance and entropy balance on the thermoacoustic device. DeltaEC [8] was used as a verification tool for this algorithm.

Srikitsuwan et al. [9] suggested genetic algorithms as an optimization design algorithm with two-point boundary value problem. They showed that this method is beneficial for maximization of the thermoacoustic refrigerator performance.

Zolpakar et al. [10] used the Multi-Objective Genetic Algorithm (MOGA) approach, and validated their results. Optimized normalised stack length and stack porosity for a thermoacoustic refrigerator were obtained, with 0.29 and 0.72 respectively.

However, a major problem of these optimization algorithms is that the clarification of the temperature difference change across the stack is not provided. Moreover, the operating conditions are chosen at the primary design steps, and then they remain constant. Maximizing the refrigerator performance is the main goal of the optimization process without taking into consideration the temperature difference across the stack or taking into account adjusting the operating condition to the new arrangements.

There is a large volume of published studies addressing the role of the geometric parameters on the performance of the thermoacoustic refrigerator [11–20]. Studies such as conducted by Zolpakar et al. [11] have shown that the geometric parameters of the stack have an impact on

the temperature difference across it. Thus, they influence the whole performance of the thermoacoustic refrigerator. The thermal performance of different stack materials was experimentally studied by Yahya et al. [17]. The stacks from the steel wool material witnessed the best performance. Nayak et al. [20] studied the performance of a thermoacoustic refrigerator using different stack geometry, and under different operating conditions. They showed the effect of different operating conditions on the temperature difference. Despite of these studies importance, the geometric parameters that compromise both the temperature difference and the performance of the thermoacoustic refrigerator were not investigated.

Operating conditions are substantial for the thermoacoustic refrigerator performance. Some researchers have already drawn attention to the importance of the operating conditions in their studies, such as Wantha and Assawamartbunlue [21] who experimentally investigated the resonance frequency change, as a result of the loudspeaker back volume change. The increase and the decrease of the back-volume size changed the resonance frequency. Nsofor and Ali [22] built an experimental thermoacoustic refrigerator to show the effect of changing the cooling load on the performance. They recommended certain frequency and pressure for the system best performance. Prashantha et al. [23] studied a thermoacoustic refrigerator operating using DeltaEC at mean pressure from 1 to 10 bar. For helium as a working fluid and 10 W, the 3 % drive ratio was found better than operating at 2 % drive ratio.

The studies about the operating conditions have mainly focused on its change with the temperature difference across the stack or the performance. However, much uncertainty still exists about the relation between the operating conditions, and both the temperature difference across the stack and the performance of the thermoacoustic refrigerator.

Overall, the operating conditions and geometric parameters affect the temperature difference across the stack and the performance of a thermoacoustic refrigerator. There is a lack of information about how the operating conditions and geometric parameters can be compromised to give the highest performance and temperature difference across the stack.

The main contributions of this paper are:

- To investigate the operating conditions and geometric parameters effect on the performance and the temperature difference across the stack.
- To get optimized values of the operating conditions and geometric parameters that compromise both the performance and the temperature difference across the stack.

The present study offers some important insights into the relationship between the geometric parameters (namely, stack position, stack length and stack spacing) and the operating conditions (namely, mean pressure and amplitude pressure), and their effect on the thermoacoustic refrigerator performance and the temperature difference across the stack, also it provides a physical demonstration to this relationship.

2. Thermoacoustic Refrigerator Design

The thermoacoustic effect occurs inside the stack walls, so the thermal contact and viscous losses are presented at the stack surface. The thermal penetration depth δ_k is the gas layer thickness where heat is transferring through during half a cycle of vibrations [5]:

$$\delta_k = \sqrt{\frac{2K}{\omega \rho_m c_p}} \tag{2}$$

Viscous penetration depth δ_v is the layer thickness where viscosity effect is observable across the boundaries [5]:

$$\delta_v = \sqrt{\frac{2\mu}{\omega \rho_m}} \tag{3}$$

The thermoacoustic refrigerator design parameters number is large to be used in thermoacoustic refrigerator equations, so a normalised analysis as shown in Table 1 for thermoacoustic design parameters was presented by Wetzel et. al [5].

Insert Table 1 about here.

The stack geometric parameters influence the gained cooling load and the needed input power as demonstrated in Eqn. 4 and Eqn. 5 for the normalised cooling power $\dot{Q}_{cn}$ and the normalised acoustic power $\dot{W}_n$ respectively. The coefficient of performance (C.O.P) is defined as the ratio of the obtained cooling power to the consumed acoustic power.

$$\dot{Q}_{cn} = -\frac{\delta_{kn} D^2 \sin(2X_{sn})}{8\gamma\Lambda(1+\sigma)} \left[\frac{\Delta T_{mn} \tan(X_{sn})}{L_{sn} B(\gamma-1)} \frac{1+\sqrt{\sigma}+\sigma}{1+\sqrt{\sigma}} - \left(1 + \sqrt{\sigma} - \sqrt{\sigma}\delta_{kn}\right) \right] \tag{4}$$

$$\dot{W}_n = \frac{\delta_{kn} L_{sn} D^2}{4\gamma} (\gamma - 1) B \cos^2(X_{sn}) \left(\frac{\Delta T_{mn} \tan(X_{sn})}{\Lambda L_{sn} B(\gamma-1)(1+\sqrt{\sigma})} - 1\right) - \frac{\delta_{kn} L_{sn} D^2}{4\gamma} \frac{\sqrt{\sigma} \sin^2(X_{sn})}{\Lambda B} \tag{5}$$

Where: $$\Lambda = 1 - \frac{\delta_v}{y_0} + \frac{{\delta_v}^2}{2\,{y_0}^2} \quad (6)$$

An initial design of thermoacoustic refrigerator depending on the sequence showed in Fig. 2 is presented [6]. A low-amplitude standing wave thermoacoustic refrigerator design is chosen to give a desired temperature difference across the stack, $\Delta T_m = 15\ \mathrm{K}$, mean operating temperature, $T_m = 300\ \mathrm{K}$, a primary cooling power of $5\ \mathrm{W}$, mean pressure, $p_m = 2\ \mathrm{bar}$, pressure amplitude, $p_o = 2\ \mathrm{kPa}$ and frequency, $f = 500\ \mathrm{Hz}$ using helium. The parallel plate stack from Mylar material is selected with porosity 0.75. The resonator is selected from a PVC material which can reduce the thermal losses at the desired temperature difference across the stack [1]. The obtained results from the design steps are used in the DeltaEC model.

Insert Fig. 2 about here.

3. DeltaEC Model

The effect of the operating conditions and geometric parameters change on the coefficient of performance of the thermoacoustic refrigerator and the temperature difference across the stack at different cooling loads will be presented numerically with the help of the free simulation software DeltaEC version 6.3b11 [8].

Fig. 3 shows the sequence that DeltaEC uses for solving Thermoacoustics related models. DeltaEC solves the pressure and flow rate equations, which are concluded from the momentum equation and the continuity equations of fluid mechanics, respectively. Sometimes, other equations such as the energy equations are combined with the momentum equation and the continuity equations for some segments. These equations are integrated numerically along the x coordinate that starts at the Beginning segment from the left end of the resonator as shown in Fig. 1. A number of trials are then performed to form solutions for $p_1(x)$ and $U_1(x)$ that make guesses meet targets. For each segment, DeltaEC has a more complicated momentum and continuity equations that include additional effects such as the viscous and thermal losses resulting from the acoustic power dissipation at the sides of ducts; however, the general form is as following [8]:

$$\frac{dp_1}{dx} = F_{Momentum}(P_1, U_1, \rho_m, \omega, T_m, \theta, geometry, gas\ properties, solid\ properties, etc.) \quad (7)$$

$$\frac{dU_1}{dx} = F_{Continuity}(P_1, U_1, \rho_m, \omega, T_m, \theta, geometry, gas\ properties, solid\ properties, etc.) \quad (8)$$

In this study, the incoming acoustic power varies with changing the operating conditions, and geometric parameters. A known cooling load is also applied to the cold heat exchanger. The boundary conditions in the DeltaEC model at the Beginning segment (x=0) are:

- Phases of particles' pressure amplitude and flow rate are: θ (p) = θ (U) = 0.
- Pressure amplitude is constant: P_1 = 2 kPa.

The first boundary condition is to enforce the occurrence of resonance frequency [8,24] through the resonator, while the second boundary condition keeps pressure amplitude with known value independent of each trial of DeltaEC.

Insert Fig. 3 about here.

Four targets and four guesses are considered for the current model. Two targets for the volume flow rate, which will enforce complex flow rate equals to zero at the bottom end of the model, appropriate for the closed end of the resonator. The third target is a total outside energy flow equals zero, so that the model is insulated.The fourth target is a constant hot heat exchanger temperature of 303 K. Temperature of the hot heat exchanger is kept constant to show how the cold temperature is lower than this specific temperature. The four unknown guesses are the unknown hot heat exchanger power required for each DeltaEC trial, the resonance frequency (which varies with the operating conditions and geometric parameters in each trial [6,21]), volume flow rate and the mean temperature (that are dependent on the power of the acoustic driver [8], which is variant in this study) at the beginning segment.

4. Results and Discussion

The effect of different operating conditions and geometric parameters on both the temperature difference across the stack and the performance of a thermoacoustic refrigerator is presented. After that, a compromise is held for maximizing both the temperature difference across the stack and the performance according to the criteria of acceptable range shown in Table 2. These criteria are considered reasonable for the required design parameters demonstrated in Section 2, which were primarily for small-size refrigerators. After that, the compromised values for the operating conditions and geometric parameters were chosen to achieve two factors. First, the values of the operating conditions and geometric parameters fall in the shown range in table 2 for the different parameters. Second, the operating conditions and geometric parameters have values in between high performance and high temperature difference across the stack.

Insert table 2 about here.

4.1 Mean Pressure

Increasing the mean pressure decreases the temperature difference as shown in Fig. 4a, as the pressure amplitude would be insignificant relative to the mean pressure. Further, increasing the mean pressure will increase the gas density and will change the gas properties, so it will decrease the gas thermal penetration depth, δ_k as shown in Fig. 5. The small thermal penetration depth decreases the temperature difference of the heat transfer between the gas parcels and the stack plates, as more gas parcels will be oscillating without interacting with the

stack walls. Also, increasing cooling load will lead to a decrease of the temperature difference due to the cold side temperature rise.

The acoustic energy is directly proportional to drive ratio, D, as the least wave amplitude from the input driver will lead to a good fluctuation. So, increasing mean pressure will decrease the drive ratio leading to the decrease of acoustic power, and thus increasing the performance. This is well illustrated for different cooling loads at Fig. 4b. Moreover, increasing the cooling power will increase the coefficient of performance.

Insert Fig.4 about here.

Insert Fig. 5 about here.

The mechanical strength of the resonator tubes is an important factor due to the resonator must withstand the high-pressure values; also, there will be a vibrational effect at high pressure and manufacture problems due to leak of the working gas at high pressures.The mean pressure effect on both the performance and the temperature differences across the stack is studied and the manufacture limits is added to this study. Then, a compromise is made to select the suitable mean pressure for our design considering the acceptable range in Table 2. After compromise, a mean pressure of 2 bar is selected.

4.2 Amplitude Pressure

The temperature difference starts at a low value in the first part of Fig. 6a due to the weakness of the pressure amplitude to make the change. After that, the increase of amplitude pressure increases the temperature difference, until it reaches a maximum value obtained near a drive ratio of 3 %.

The consumed acoustic energy is proportional to the drive ratio. The input acoustic energy for a fixed mean pressure increases with the acoustic pressure increase, which means a lower performance as shown in Fig. 6b.

Insert Fig. 6 about here.

The maximum temperature difference occurs at drive ratio equals 3%, but the performance is another key parameter and we considered factors shown in table 2. Therefore, a drive ratio equals 2 % is chosen to improve the performance and to account for the driver abilities to provide that drive ratio.

4.3 Stack Position

The input acoustic signal changes with a sine wave, so the temperature distribution is also changed. The temperature difference gives a peak value at a normalised stack position, X_{sn} = 0.25 as shown in Fig. 7a, although the performance is maximum at a normalised stack position, X_{sn} = 0.3 as shown in Fig. 7b. The values of temperature differences at normalised stack positions from 0.25 to 0.3 do not change with a sensible change, so a normalised stack position equals 0.3 is chosen.

Insert Fig. 7 about here.

4.4 Stack Length

Increasing the stack length means that larger number of the working fluid molecules will interact with the stack plates leading to the increase of temperature difference as shown in Fig. 8a. The stack is the place where the thermoacoustic effect and pumping heat takes place, so increasing the stack length will lead to more gas particles interact with the stack plates, and thus the acoustic power consumption will increase, and the performance will decrease as shown in Fig. 8b. However, further increasing the stack length will result in a decrease in the temperature difference across the stack. This observed decrease in temperature difference across the stack could be attributed to the variability of the acoustic field inside the resonator. This means that shorter stack lengths will experience linear temperature gradient across the stack, while longer stack lengths could interfere with the acoustic field at low-pressure areas leading to non-linear distribution of the temperature gradient through the stack length.

The increase of the normalised stack length will cause the temperature difference to increase, but also will lead to a massive drop on the coefficient of performance. A compromise is executed choosing a normalised stack length equals to 0.12, and this will increase performance to 1.32 and a decrease of temperature difference to 31 K at a cooling load of 5 W.

For different stack positions and cooling load of 5 W, the normalised stack length effect on the temperature difference and the coefficient of performance will be as shown in Fig. 9. The peak values for the temperature difference for different stack lengths will be at different stack positions.

Insert Fig. 8,9 about here.

4.5 Stack Spacing

The thermal and viscous penetration depths parameters make a deep understanding of plate spacing change effect. In the first part of Fig. 10a, it shows the temperature difference across the stack when the spacing is so small, the viscous losses will play a major role on the boundaries of the plates at this stage. Thus, increasing the spacing between the plates reduces the viscous penetration depth effect and the viscosity losses. So, the temperature difference will increase gradually, until reaching the peak at spacing approximately equals to $3\ \delta_k$. After that, a weak thermal interaction with the plates is observed with the increase in the stack spacing, and the temperature difference is then considerably decreased.

Increasing the plate spacing will increase the coefficient of performance in the studied range of normalized stack spacing, as the viscous losses are declined leading to a significant decrease in the consumed acoustic power and higher heat transfer rates between the gas particles and the cold heat exchanger according to the results obtained by DeltaEC. Until it reaches a region, where the change is less sensitive and the performance will remain constant as shown in Fig. 10b.

A spacing to thermal penetration depth of 4 compromises the performance and the temperature difference, as the temperature is nearly maximum and the performance is still increasing. This stack spacing results in a final temperature difference across the stack of 29.5 K and a C.O.P. of 1.24 at a cooling load of 5 W.

Insert Fig. 10 about here.

5. Conclusion

Theoretical study using DeltaEC is presented to show the effect of changing the geometric parameters and operating conditions of a thermoacoustic refrigerator on both the coefficient of performance and the temperature difference across the stack. In addition, the physical phenomenon of the effect of the operating conditions and the geometric parameters is introduced. Moreover, depending on the designed thermoacoustic refrigerator, compromised values for the operating conditions and geometric parameters are collected as following:

- A drive ratio of 2 % will compromise the temperature difference and the coefficient of performance.
- A normalised stack position of 0.3 will compromise both the temperature difference across the stack and the performance.
- Increasing the stack length will increase the temperature difference, but this also will make the power consumption higher, and thus leads to a lower performance. A normalised stack length of 0.12 is chosen for such compromise.
- A spacing to thermal penetration depth value of 4 compromise the performance and the temperature difference.

These findings enhance our understanding of the variations of the temperature difference across the stack and the performance of a thermoacoustic refrigerator with the geometric parameters and the operating conditions.

Nomenclature

Latin Letters

A	Resonator area, $[m^2]$
a	Sound velocity, $[m/s]$
B	Porosity, …
c	Specific heat, $[kJ/\ (kg.K)]$
D	Drive ratio, …
f	Frequency, $[Hz]$
K	Thermal conductivity, $[W/\ (m.K)]$
L	Length, $[m]$
l	The half plate thickness, $[mm]$
P	Pressure, $[Pa]$
$\dot{Q}$	Thermal power, $[kW]$
T	Temperature, $[K]$
U	Particle flow rate, $[m^3/s]$
$\dot{W}$	Acoustic power, $[kW]$
X	Stack position, $[m]$
y_o	Half stack spacing, $[mm]$

Greek Letters

ε_s	Stack heat capacity ratio, …
γ	Ratio of specific heats, …
δ_k	Thermal penetration depth, $[m]$
δ_v	Viscous penetration depth, $[m]$
λ	Wave length, $[m]$
μ	Dynamic viscosity, $[Pa.s]$
ρ	Fluid density, $[kg/m^3]$
σ	Prandtl numbe, …
ω	Angular frequency, $[rad/s]$
ΔT	Temperature Difference, $[K]$

Subscripts

1	Amplitude or oscillatoryc
Cold	
hex	Heat exchanger
k	Thermal
m	Mean
n	Normalized
p	At constant pressure
res	Resonator
s	Stack
tot	Total
v	Viscous

References

[1] Zolpakar NA, Mohd-Ghazali N, Hassan El-Fawal M. Performance analysis of the standing wave thermoacoustic refrigerator: A review. Renew Sustain Energy Rev 2016;54:626–34. doi:10.1016/j.rser.2015.10.018.

[2] Paek I, Braun J, Mongeau L. Evaluation of standing-wave thermoacoustic cycles for cooling applications. Int J Refrig 2007;30:1059–71.

[3] Brown J, Domanski P. Review of alternative cooling technologies. Appl Therm Eng 2014;64:252–62.

[4] Tassou S, Lewis J, Ge Y, Hadawey A. A review of emerging technologies for food refrigeration applications. Appl Therm Eng 2010;30:263–76.

[5] Wetzel M, Herman C. Design optimization of thermoacoustic refrigerators. Int J Refrig 1997;20:3–21.

[6] Tijani M. Loudspeaker-driven thermo-acoustic refrigeration. 2001.

[7] Babaei H, Siddiqui K. Design and optimization of thermoacoustic devices. Energy Convers Manag 2008;49:3585–98. doi:10.1016/j.enconman.2008.07.002.

[8] Clark JP, Ward WC, Swift GW. Design environment for low-amplitude thermoacoustic energy conversion (DeltaEC) Version 6.3 b11 Users Guide. 2012.

[9] Srikitsuwan S, Kuntanapreeda S, Vallikul P. A genetic algorithm for optimization design of thermoacoustic refrigerators. Proc 7th WSEAS Int Conf Simul 2007.

[10] Zolpakar NA, Mohd-Ghazali N, Ahmad R. Experimental investigations of the performance of a standing wave thermoacoustic refrigerator based on multi-objective genetic algorithm optimized parameters. Appl Therm Eng 2016;100:296–303. doi:10.1016/j.applthermaleng.2016.02.028.

[11] Zolpakar NA, Mohd-Ghazali N. Optimization of the Stack Unit in a Thermoacoustic Refrigerator. Heat Transf Eng 2017;38:431–7.

[12] Tartibu LK. Maximum cooling and maximum efficiency of thermoacoustic refrigerators. Heat Mass Transf Und Stoffuebertragung 2016;52:95–102. doi:10.1007/s00231-015-1599-y.

[13] Alcock AC, Tartibu LK, Jen TC. Experimental Investigation of Ceramic Substrates in Standing Wave Thermoacoustic Refrigerator. Procedia Manuf 2017;7:79–85. doi:10.1016/j.promfg.2016.12.021.

[14] Tasnim S, Mahmud S, Fraser R. Modeling and analysis of flow, thermal, and energy fields within stacks of thermoacoustic engines filled with porous media. Heat Transf Eng 2013;34:84–97.

[15] Ibrahim A, Omar H, Abdel-Rahman E. Constraints and challenges in the development of loudspeaker-driven thermoacoustic referierator. Proc. 18th Int. Congr. Sound Vib., 2011.

[16] Hariharan N, Sivashanmugam P. Experimental investigation of a thermoacoustic refrigerator driven by a standing wave twin thermoacoustic prime mover. Int J Refrig 2013;36:2420–5.

[17] Yahya S, Mao X, Jaworski A. Experimental investigation of thermal performance of random stack materials for use in standing wave thermoacoustic refrigerators. Int J Refrig 2017;75:52–63.

[18] Elnegiry E, Eltahan H, Alamir M. Optimizing the performance of a standing wave loudspeaker driven thermoacoustic heat pump. Int J Sci Eng Res 2016;7:460–5.

[19] Zoontjens L, Howard C. Development of a low-cost loudspeaker-driven thermoacoustic refrigerator. Proc Acoust 2005.

[20] Nayak B, Pundarika G, Arya B. Influence of stack geometry on the performance of thermoacoustic refrigerator. Sādhanā 2017:1–8.

[21] Wantha C, Assawamartbunlue K. Experimental investigation of the effects of driver housing and resonance tube on the temperature difference across a thermoacoustic stack. Heat Mass Transf Und Stoffuebertragung 2013;49:887–96. doi:10.1007/s00231-013-1150-y.

[22] Nsofor E, Celik S, Wang X. Experimental study on the heat transfer at the heat exchanger of the thermoacoustic refrigerating system. Appl Therm Eng 2007;27:2435–42.

[23] Prashanthaa B, Gowdab M, Seetharamuc S. Effect of mean operating pressure on the performance of stack-based thermoacoustic refrigerator. Int J Therm Environ Eng 2013;5:83–9.

[24] Tijani MEH, Zeegers JCH, De Waele ATAM. Design of thermoacoustic refrigerators. Cryogenics (Guildf) 2002;42:49–57. doi:10.1016/S0011-2275(01)00179-5.

Table 1
Normalised Parameters of the thermoacoustic refrigerator.

Normalised design requirements		**Geometric parameters**	
Design parameter	Definition	Design parameter	Definition
Normalised cooling load	$\dot{Q}_{cn} = \frac{\dot{Q}_c}{P_m a A}$	Normalised stack length	$L_{sn} = \frac{L_s}{\lambda/2\pi}$
Normalised acoustic power	$\dot{W}_n = \frac{\dot{W}}{P_m a A}$	Normalised stack position	$X_{sn} = \frac{X_s}{\lambda/2\pi}$
Drive ratio	$D = \frac{P_0}{P_m}$	Blockage ratio or porosity	$B = \frac{y_0}{y_0 + 1}$
Normalised temperature difference	$\Delta T_{mn} = \frac{\Delta T_m}{T_m}$	Normalised thermal penetration depth	$\delta_{kn} = \frac{\delta_k}{2y_0}$

Table 2
Criteria for acceptable ranges of the operating conditions and geometric parameters used in this study.

Design Parameters	**Acceptable range**	**Suitability of the selected range for the used design**
Mean pressure, P_m	1:3 bar	• Materials of most available resonators like PVC resonator can withstand this pressure. • Not too high, so there is no leakage of the working fluid to outside the resonator. • Not too low, so the performance can be relatively high.
Drive ratio, D	1:2%	• Available drivers such as commercial loudspeakers will be capable of producing these drive ratios. • Large non-linearity effects might occur at D ≥ 3%, also in that range turbulence can be avoided [6].
Normalised stack length, L_{sn}	0.1:0.2	• Shorter stacks could be difficult for manufacturing. • Longer stacks can be inefficient due to their interaction with the acoustic field.
Normalised stack position, X_{sn}	0.2:0.4	• This range is close to pressure antinodes. • Shorter stack positions will be too close to the loudspeaker leading to significant viscous and thermal losses, and difficulties will be attained because stack lengths must have specific small dimensions. • Longer stack positions are close to the pressure nodes.
Normalised stack spacing, $\frac{2y_0}{\delta_k}$	2:4	• This range reduces both thermal and viscous losses and gives good heat transfer between the stack and gas particles [5].
Coefficient of performance, $C.O.P$	1:1.5	• Acceptable range for small-size refrigerators compared to conventional refrigeration systems.
Temperature difference across the stack, ΔT_m	15:30 K	• It is suitable for small-size refrigerators used in this study.

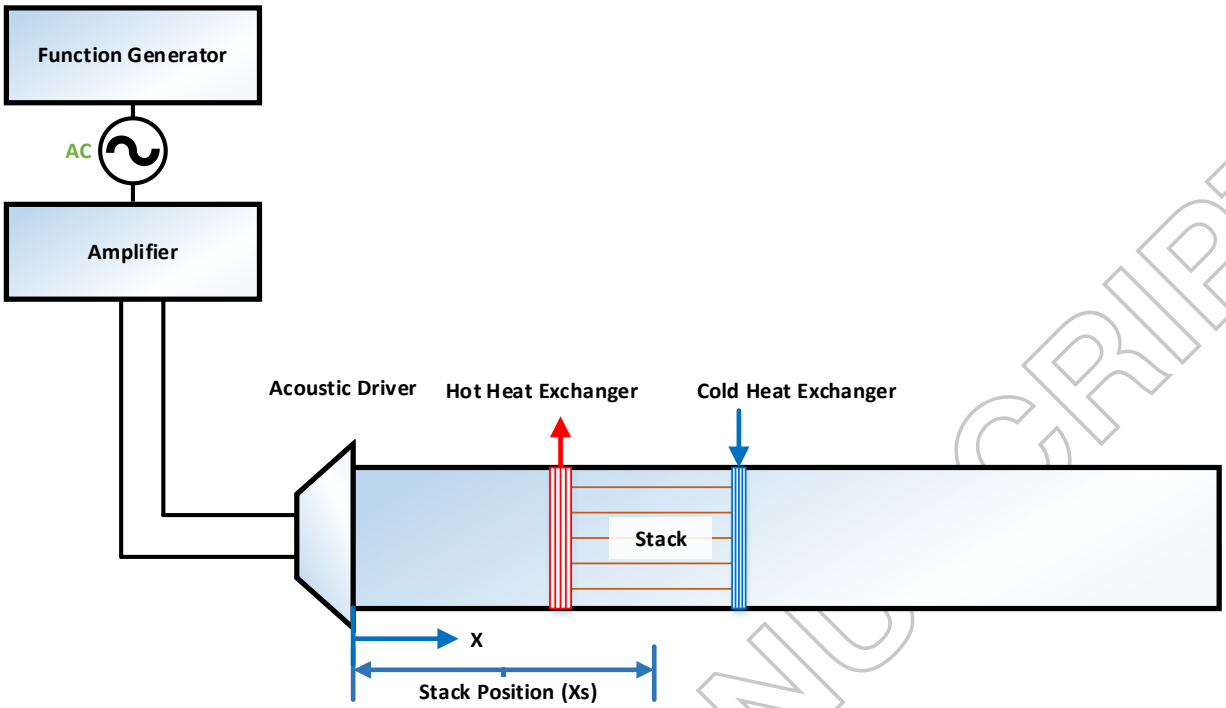

Fig. 1. A schematic diagram of standing wave thermoacoustic refrigerator components.

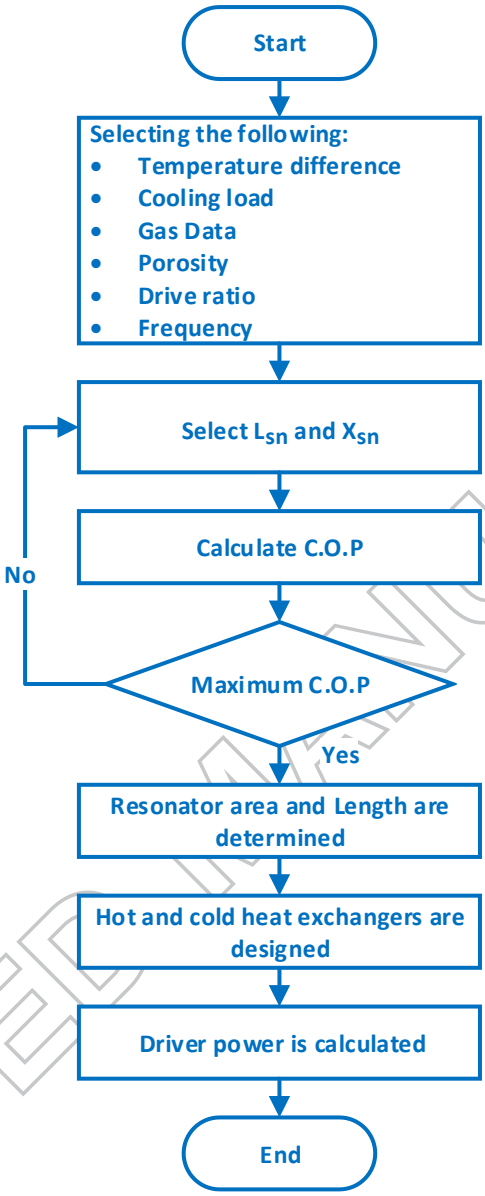

Fig. 2. Design steps for a thermoacoustic refrigerator.

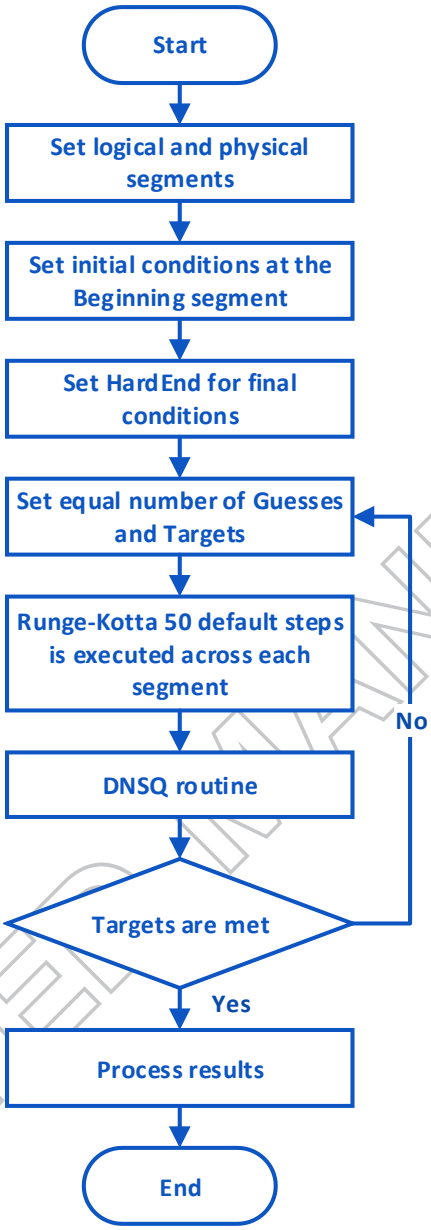

Fig. 3. DeltaEC working principle.

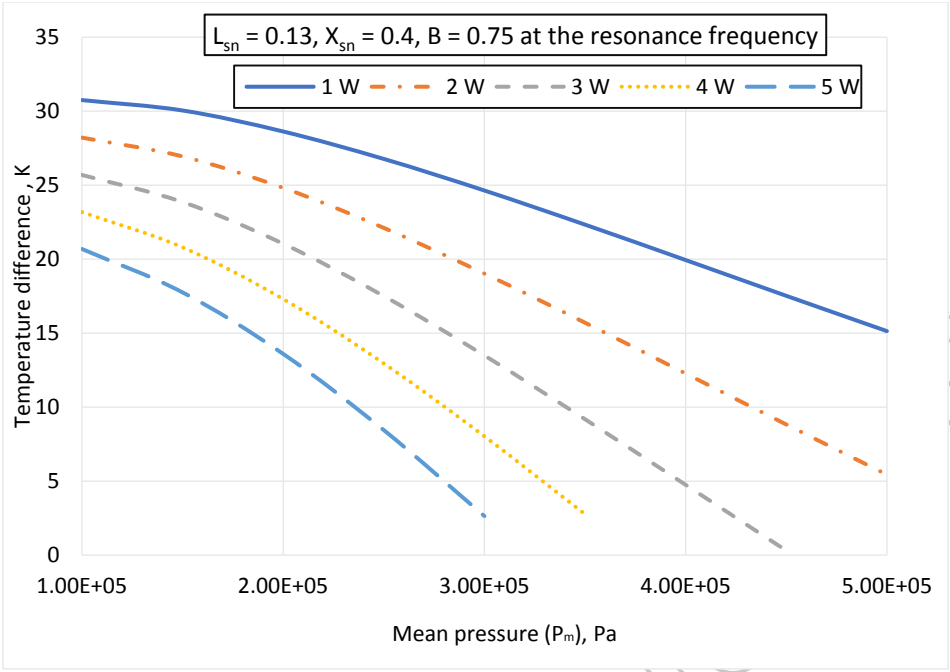

(a)

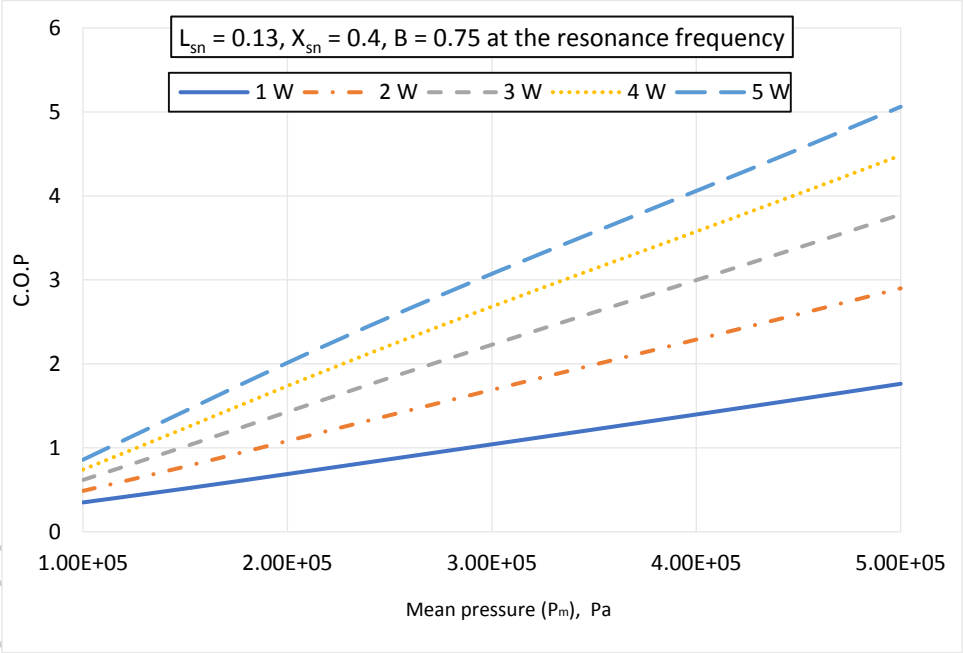

(b)

Fig. 4. Mean pressure effect on (a) Temperature difference (b) Coefficient of performance.

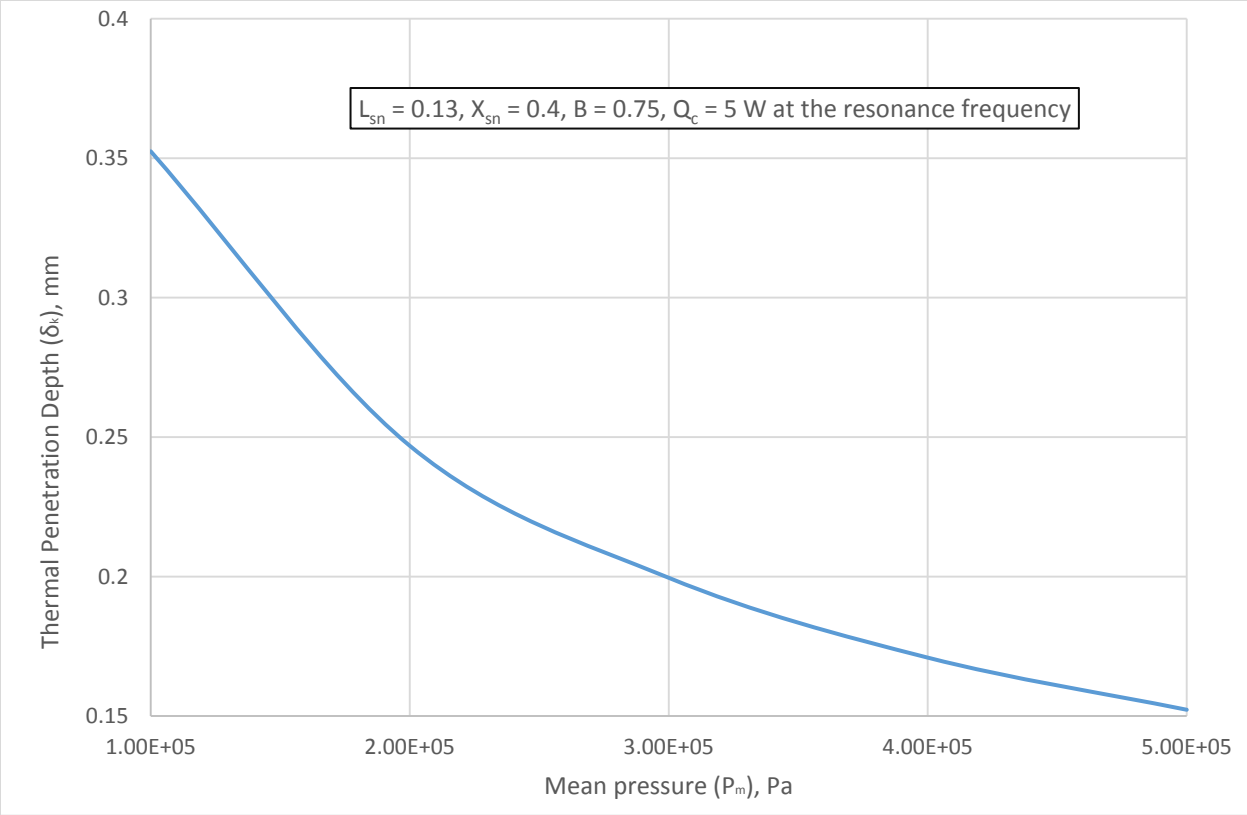

Fig. 5. Mean pressure effect on thermal penetration depth.

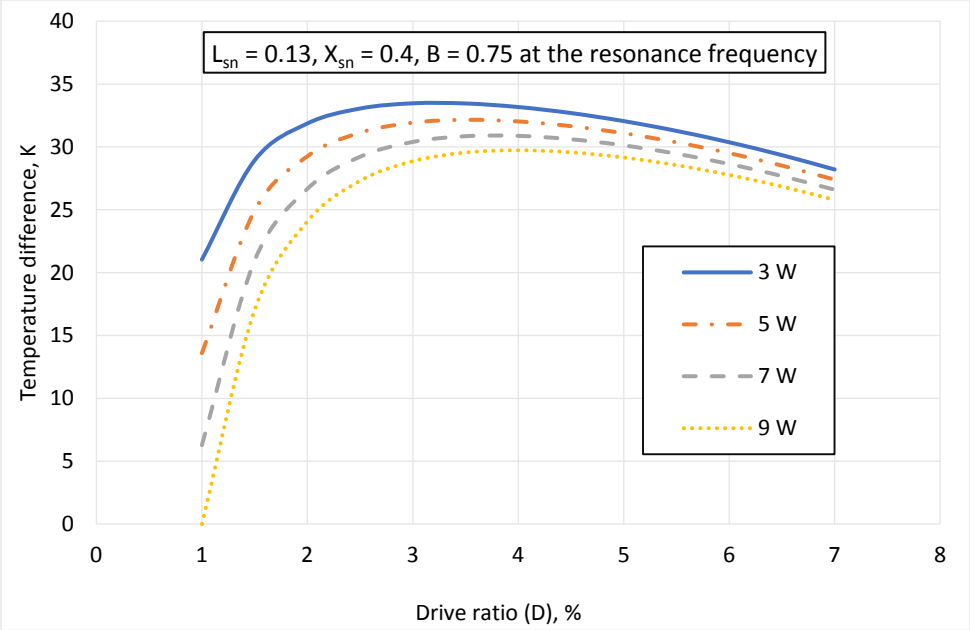

(a)

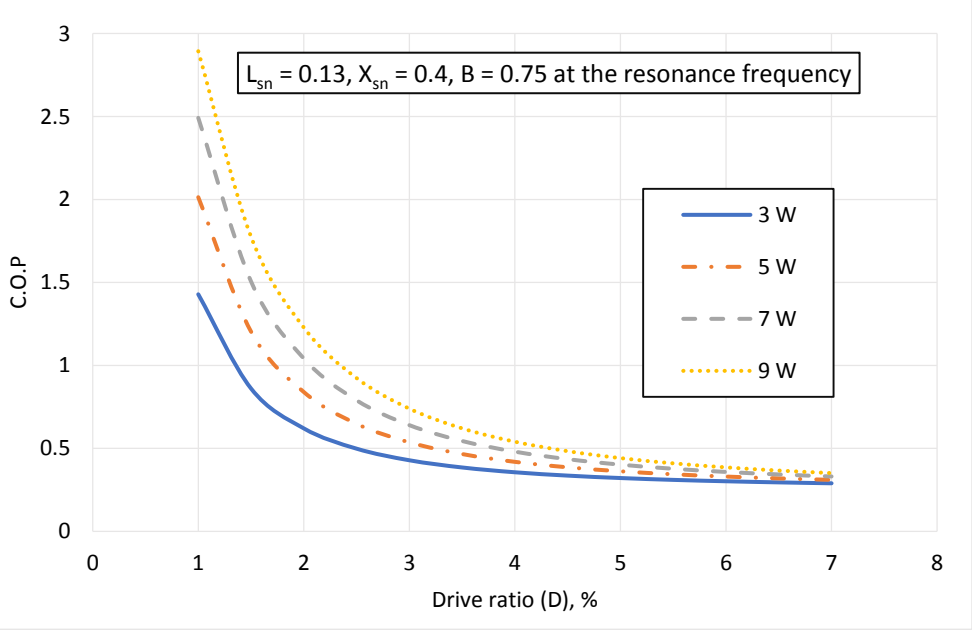

(b)

Fig. 6. The drive ratio effect on (a) Temperature difference (b) Coefficient of performance.

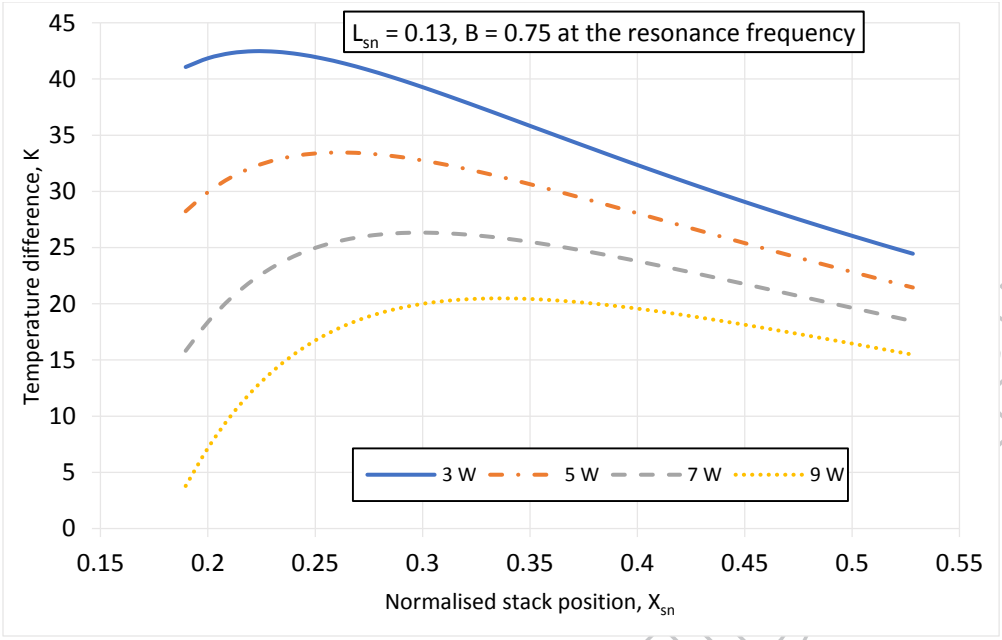

(a)

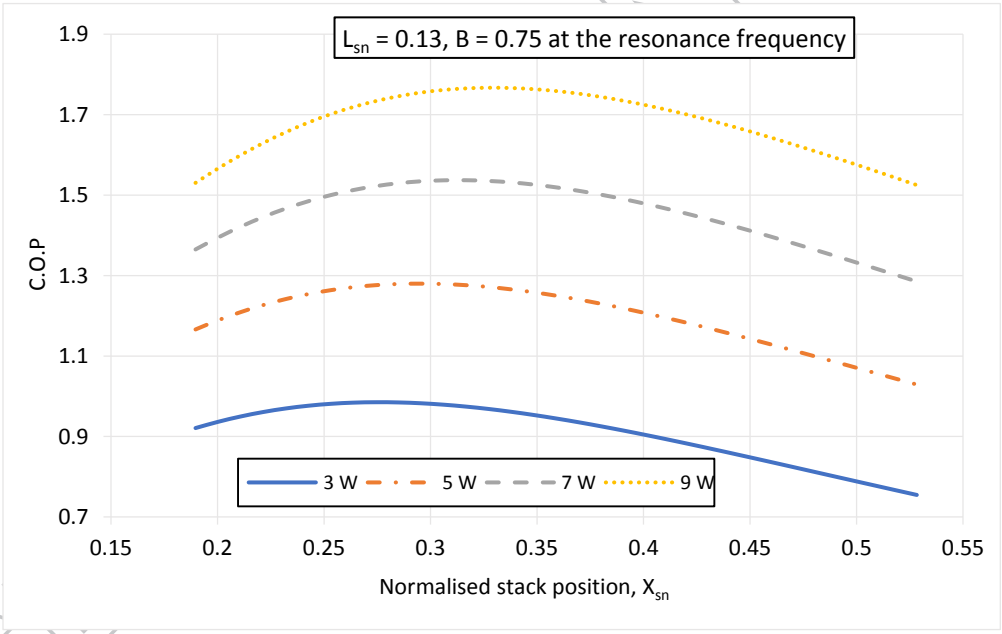

(b)

Fig. 7. The normalised stack position effect (a) Temperature difference (b) Coefficient of performance.

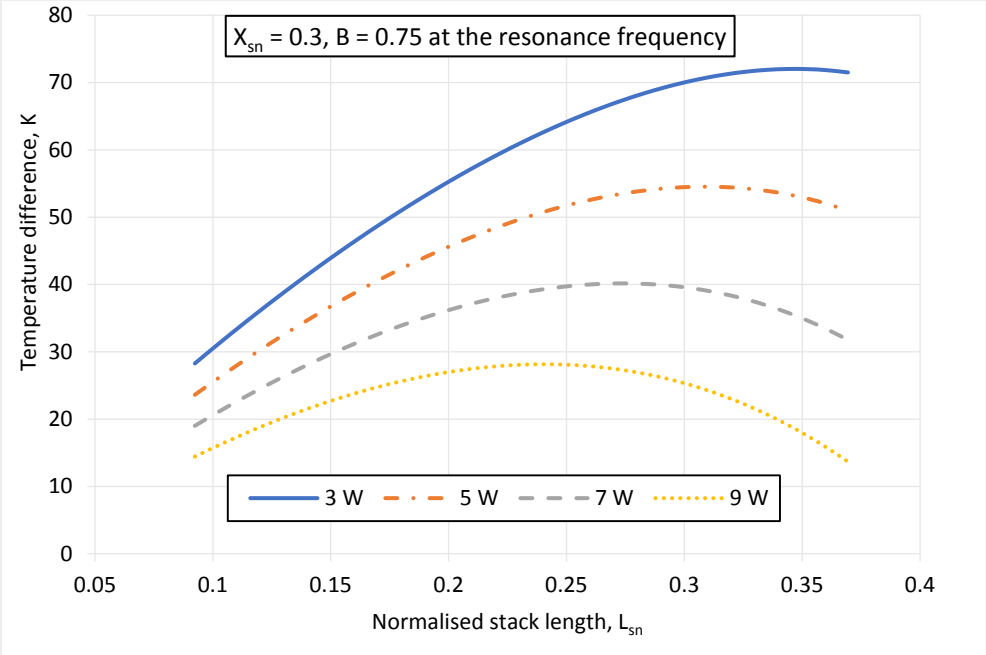

(a)

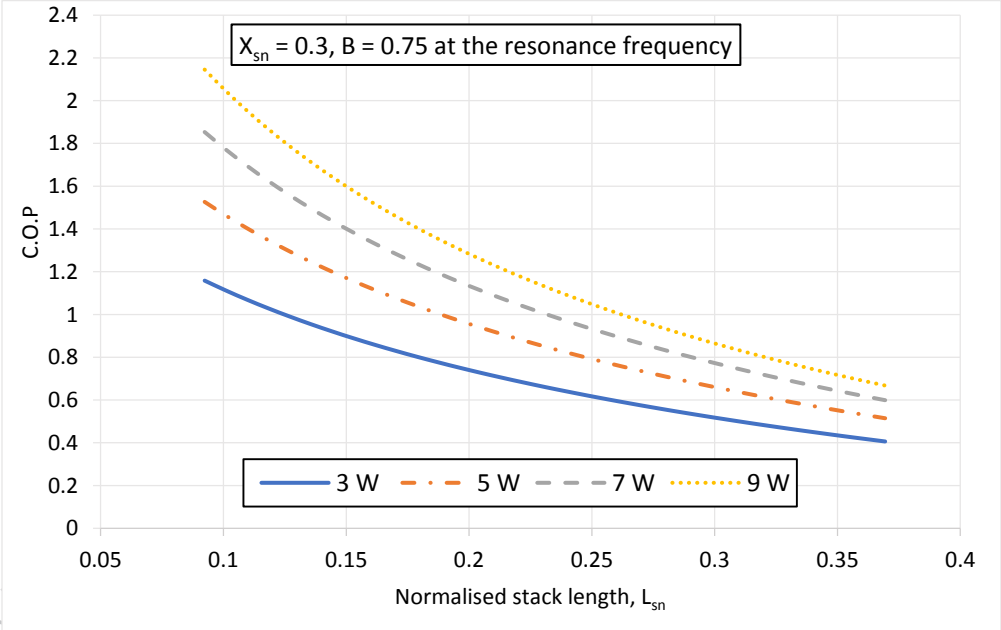

(b)

Fig. 8. The normalised stack length effect on (a) Temperature difference (b) Coefficient of performance.

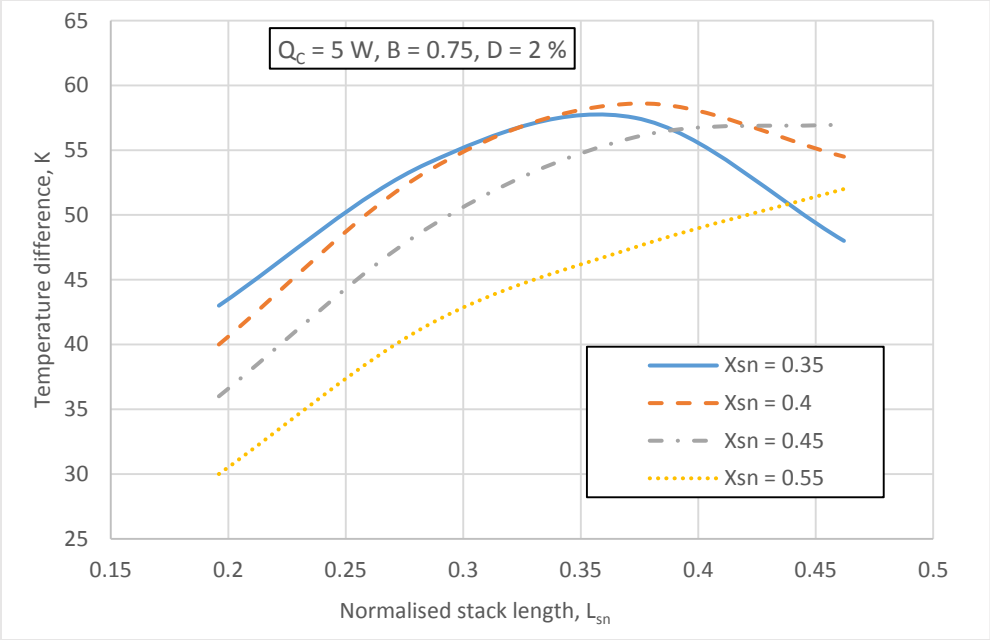

(a)

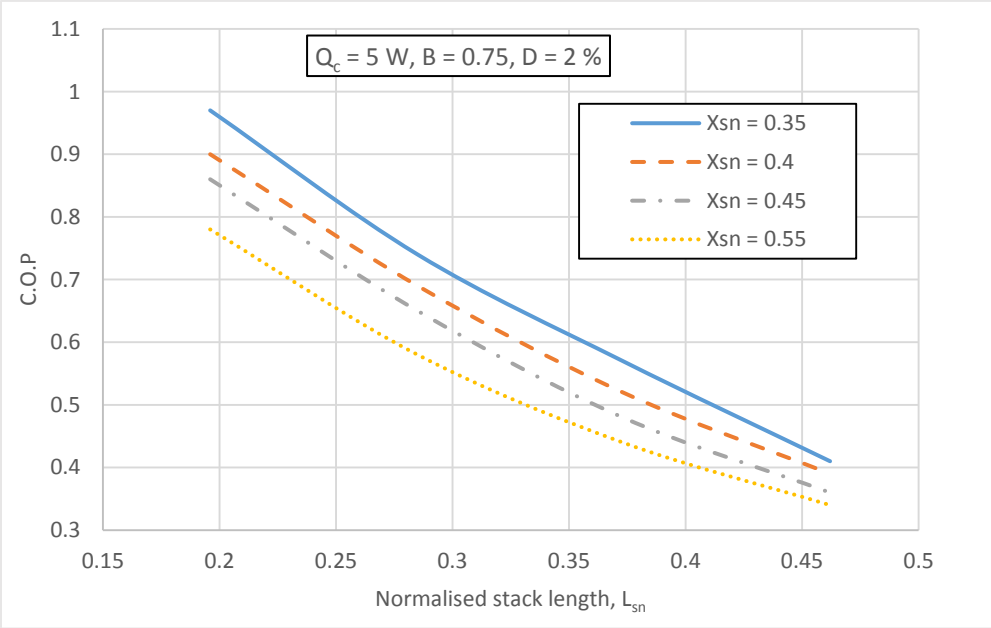

(b)

Fig. 9. Normalised stack length at different normalised stack positions effect on a) Temperature difference b) Coefficient of performance.

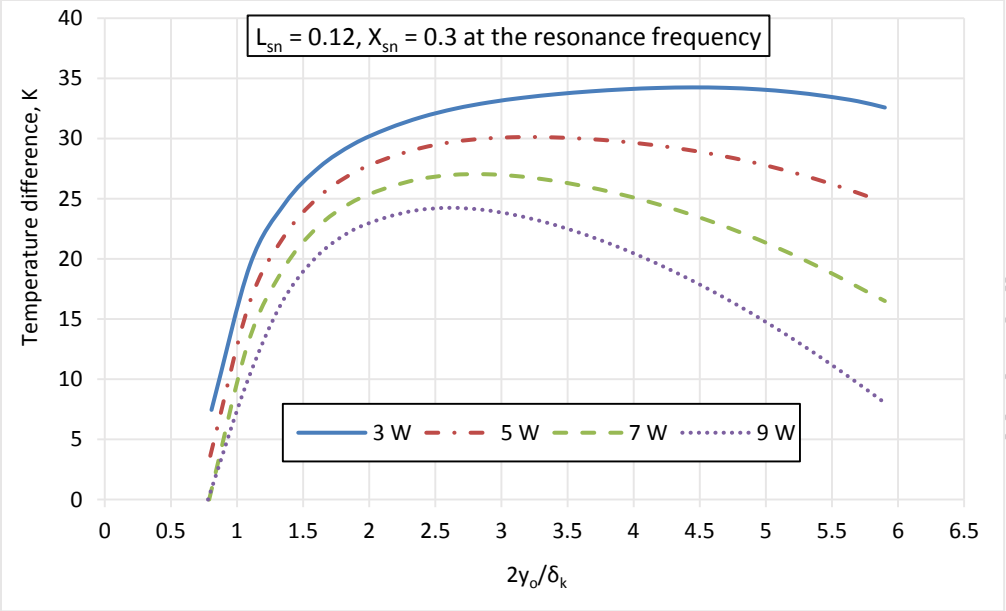

(a)

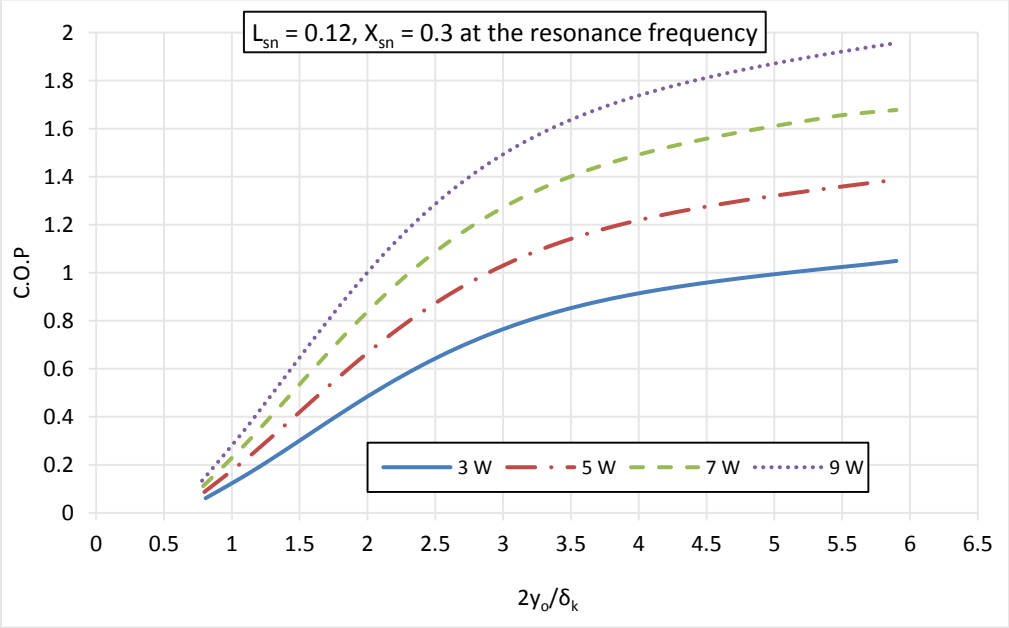

(b)

Fig. 10. The stack spacing to thermal penetration depth effect on (a) Temperature difference (b) Coefficient of performance.